

# Time evolution and matter wave interference in Fermi condensates

Wei Zhang and C. A. R. Sá de Melo

*School of Physics, Georgia Institute of Technology, Atlanta, Georgia 30332*

(Dated: January 30, 2019)

We discuss matter wave interference of Fermi condensates in strongly coupled  $s$ -wave and  $p$ -wave channels and the time evolution of a single cloud upon release from trap. In  $s$ -wave systems, where the order parameter is a complex scalar, we find that the interference patterns depend on the relative phase of the order parameters of the condensates. In  $p$ -wave systems involving the mixture of two-hyperfine states, we show that the interference pattern exhibits a polarization effect depending on the relative orientation of the two vector order parameters. However, in  $p$ -wave systems involving a single hyperfine state, we show that this angular effect reduces to an overall phase difference between the two interfering clouds, similar to  $s$ -wave. Lastly, we also point out that  $p$ -wave Fermi condensates exhibit an anisotropic expansion, reflecting the spatial anisotropy of the underlying interaction between fermions and the orbital nature of the vector order parameter.

PACS numbers: 03.75.Ss, 03.75.-b, 05.30.Fk

Matter-wave interference is a very powerful tool to study quantum phase coherence between atomic Bose Einstein condensates (BEC) [1, 2], and spatial quantum noise of bosons in optical lattices [3]. Similar techniques can also be applied to study Fermi condensates, [4, 5, 6, 7, 8, 9] where superfluidity can be tuned from the BCS to the BEC regime. These experiments may reveal that the time dynamics in the BCS regime is overdamped (large Cooper pairs can decay into two atoms), while in the BEC regime it is essentially undamped (tightly bound molecules are stable) [10, 11]. Matter-wave interference experiments of  $s$ -wave Fermi condensates may be readily performed, since stable condensates already exist. For  $s$ -wave Fermi condensates in the BEC regime quantum interference effects are expected to be similar to those of atomic Bose condensates, and the interference pattern should depend essentially on the phase difference of the order parameters between two interfering clouds.

In contrast, it is more interesting to study interference effects in  $p$ -wave superfluids because of the vector nature of the order parameter. Many groups have reported some progress towards the formation of  $p$ -wave Fermi condensates in single clouds [12, 13, 14] and in optical lattices [15], where  $p$ -wave Feshbach resonances have been observed. For Feshbach resonances currently tried in single clouds atom losses have been significant, and the realization of stable  $p$ -wave condensates has not been achieved yet. However, other unexplored Feshbach resonances in single clouds may show less dramatic two-body dipolar or three-body losses as observed in optical lattices [15]. Thus, these experimental difficulties may be surpassed in the immediate future.

We discuss in this manuscript time dynamics and matter-wave interference of  $s$ -wave and  $p$ -wave Fermi condensates. Our main results are as follows. While in atomic BEC and  $s$ -wave Fermi superfluids quantum interference patterns depend essentially on the relative

phase of the two clouds, we find that in the  $p$ -wave Fermi superfluids there can also be a strong dependence on the relative angle between the two vector order parameters, thus producing a polarization effect. Furthermore, we show that  $p$ -wave Fermi condensates exhibit an anisotropic expansion, reflecting the spatial anisotropy of the underlying interaction between fermions and the orbital nature of the vector order parameter.

We consider a system of fermions with mass  $m$  in two hyperfine states (pseudospins), labeled by greek indices  $\alpha = 1, 2$ . The Hamiltonian density is (with  $\hbar = k_B = 1$ )

$$H(\mathbf{r}, t) = \psi_{\alpha}^{\dagger}(\mathbf{r}, t) \left[ -\frac{\nabla_{\mathbf{r}}^2}{2m} + U_{\text{ext}}(\mathbf{r}, t) \right] \psi_{\alpha}(\mathbf{r}, t) - \int d\mathbf{r}' [\psi_{\alpha}^{\dagger}(\mathbf{r}, t) \psi_{\beta}^{\dagger}(\mathbf{r}', t) V_{\alpha\beta\gamma\delta}(\mathbf{r} - \mathbf{r}') \psi_{\gamma}(\mathbf{r}', t) \psi_{\delta}(\mathbf{r}, t)],$$

where repeated greek indices indicates summation,  $\psi_{\alpha}^{\dagger}$  ( $\psi_{\alpha}$ ) are creation (annihilation) operators of fermions in state  $\alpha$ , and  $H(t) = \int d\mathbf{r} H(\mathbf{r}, t)$  is the Hamiltonian. The trapping potential is  $U_{\text{ext}}(\mathbf{r}, t) = \sum_{j=x,y,z} \omega_j(t) r_j^2 / 2$ , where  $\omega_j(t < 0) = \omega_{j,0}$  are constants.

The generating functional for non-equilibrium processes associated with  $H(t)$  is [16]

$$Z(t) = \text{Tr} \hat{\mathcal{U}}^{\dagger}(t, t_0) \exp[-\beta(H(t_0) - \mu_{\alpha} N_{\alpha})] \hat{\mathcal{U}}(t, t_0),$$

where  $N_{\alpha}$  is the number operator for fermions of type  $\alpha$ ,  $\mu_{\alpha}$  is the corresponding chemical potential, and  $\beta = 1/T$  is the inverse temperature. Here,  $\hat{\mathcal{U}}(t, t_0) \equiv \exp[-i \int_{t_0}^t H(t') dt']$  is the time evolution operator. This expression implicitly implies that the system is in thermal equilibrium at any time  $t_0 < 0$ , since  $Z(t_0) = \text{Tr} \exp[-\beta(H(t_0) - \mu_{\alpha} N_{\alpha})]$ . By introducing a complex time  $\tau$ , the generating functional can be written as

$$Z(t) = \int_{\text{BC}} \Pi_{\alpha} D[\psi_{\alpha}^{\dagger}, \psi_{\alpha}] e^{-i[S_2(\psi_j^{\dagger}, \psi_j) + S_4(\psi_j^{\dagger}, \psi_j)]}, \quad (1)$$

where the boundary condition (BC) of the functional integral is  $\psi_{\alpha}(\mathbf{r}, t_0 - i/T) = -\psi_{\alpha}(\mathbf{r}, t_0)$ . The quadratic

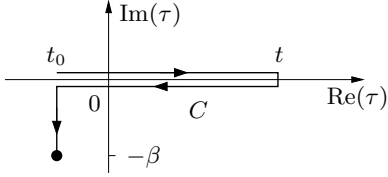


FIG. 1: Integration contour  $C$  used in Eq. (2).

term is

$$S_2(\psi_j^\dagger, \psi_j) = \int_C d\tau \int d\mathbf{r} \psi_\alpha^\dagger(\mathbf{r}, \tau) \hat{\mathcal{L}}_\alpha(\mathbf{r}, \tau) \psi_\alpha(\mathbf{r}, \tau), \quad (2)$$

where the integration contour  $C$  is shown in Fig. 1. The one-particle operator  $\mathcal{L}_\alpha$  is defined as

$$\hat{\mathcal{L}}_\alpha(\mathbf{r}, \tau) = -i\partial_\tau - \frac{\nabla^2}{2m} + U_{\text{ext}}(\mathbf{r}, \tau) - \mu_\alpha.$$

In what follows, we discuss the  $p$ -wave case in detail and quote the more standard results for  $s$ -wave. To calculate the fourth order term  $S_4$ , we write  $V_{\alpha\beta\gamma\delta}(\mathbf{x}) = V(\mathbf{x})\Gamma_{\alpha\beta\gamma\delta}$ , where in a triplet channel  $\Gamma_{\alpha\beta\gamma\delta} = \mathbf{v}_{\alpha\beta} \cdot (\mathbf{v}^\dagger)_{\gamma\delta}$ . The pseudospin matrices  $(v_j)_{\alpha\beta} \equiv (i\sigma_j\sigma_y)_{\alpha\beta}$ , where  $\sigma_j$  are Pauli matrices. This form of interaction implies that the interaction strength is the same for all pseudospin channels. (Deviations from this assumption will be discussed later). By introducing  $\mathbf{B}^\dagger(\mathbf{r}, \mathbf{r}', \tau) = \psi_\alpha^\dagger(\mathbf{r}, \tau)\mathbf{v}_{\alpha\beta}\psi_\beta^\dagger(\mathbf{r}', \tau)$  and the corresponding auxiliary field  $\mathbf{d}^\dagger(\mathbf{r}, \mathbf{r}', \tau)$ , the interaction term  $S_4$  can be decoupled via a Hubbard–Stratonovich transformation. We integrate out the fermions and write  $\mathbf{d}(\mathbf{r}, \mathbf{r}', \tau) = \sum_n \mathbf{D}_n(\mathbf{R}, \tau)\eta_n(\mathbf{x})$ , where  $\eta_n(\mathbf{x})$  are eigenfunctions of the reduced two-body Hamiltonian  $\mathcal{H}_2 = -\nabla_{\mathbf{x}}^2/m + V(\mathbf{x})$ . Here,  $\mathbf{R} = (\mathbf{r} + \mathbf{r}')/2$  and  $\mathbf{x} = \mathbf{r} - \mathbf{r}'$  are center-of-mass and relative coordinates, respectively. In strong coupling limit where the interaction is the largest energy scale in the problem (with typical strength much larger than temperature and trapping potential), the ground state of  $\mathcal{H}_2$  has the same symmetry of  $V$ . For definiteness, we consider a pure  $p$ -wave interaction where the ground state is three-fold degenerate and labeled by  $\nu = x, y, z$ , with corresponding eigenfunctions  $\eta_\nu(x)\hat{x}_\nu$ . Thus, at low temperatures where the higher energy states are not excited, we have  $\mathbf{d} = \sum_\nu \mathbf{D}_\nu(\mathbf{R}, \tau)\eta_\nu(x)\hat{x}_\nu$ .

In this strong coupling limit, Cooper pairs are tightly bound molecules and their relative degrees of freedom can be integrated out leading to

$$S_{\text{eff}} = - \int_C d\tau \int d\mathbf{R} \left\{ \mathbf{D}^\dagger(\mathbf{R}, \tau) \cdot \left[ \hat{K}\mathbf{D}(\mathbf{R}, \tau) \right] - \frac{g_0}{2} [2|\mathbf{D}(\mathbf{R}, \tau)|^4 - |\mathbf{D}^2(\mathbf{R}, \tau)|^2] \right\}, \quad (3)$$

where  $D_j(\mathbf{R}) \equiv \sum_\nu D_{j,\nu}(\mathbf{R})$  is the order parameter, and the operator  $\hat{K} = i\partial_\tau - 2U_{\text{ext}}(\mathbf{R}, \tau) + \nabla_{\mathbf{R}}^2/(4m)$  corresponds to the action of an ideal non-equilibrium gas of

Bose particles with mass  $M = 2m$ . This action leads to equations of motion

$$i\partial_t D_j = \left[ -\frac{\nabla_{\mathbf{R}}^2}{2M} + 2U_{\text{ext}}(\mathbf{R}, t) + 2g_0|\mathbf{D}|^2 \right] D_j - g_0(\mathbf{D} \cdot \mathbf{D}) D_j^\dagger. \quad (4)$$

Notice that this expression is different from the time-dependent Gross-Pitaevskii (TDGP) equation for a vector boson field. The difference comes from the last term, which describes a non-unitary complex order parameter of the underlying paired fermions. In contrast, the standard TDGP equation for scalar bosons is obtained in the  $s$ -wave case [16].

Equation (4) can be simplified to the TDGP form in two special cases. First, if two hyperfine states are equally populated and  $\mathbf{D}$  is unitary, then it can be represented by a real vector with an overall phase factor, leading to the equation of motion

$$i\partial_t D_j = \left[ -\frac{\nabla_{\mathbf{R}}^2}{2M} + 2U_{\text{ext}}(\mathbf{R}, t) + g_0|\mathbf{D}|^2 \right] D_j. \quad (5)$$

Second, if only one hyperfine state is populated, then  $\mathbf{D}$  is non-unitary and  $\mathbf{D} = A(1, -i, 0)$ , where  $A$  is a complex constant. Thus, the last term  $\mathbf{D} \cdot \mathbf{D}$  in Eq. (4) vanishes, and the equation of motion is identical to Eq. (5), with  $g_0 \rightarrow 2g_0$ . In the following discussion, we confine ourselves to these two special cases.

For definiteness, we assume that the trapped Fermi superfluid is released at time  $t = 0$ , i.e.,  $U_{\text{ext}}(t > 0) = 0$ . Thus, for  $t < 0$ , the system is described by

$$\mu_0 D_j(\mathbf{R}) = \left[ -\frac{\nabla_{\mathbf{R}}^2}{2M} + 2U_{\text{ext}}(\mathbf{R}) + g|\mathbf{D}|^2 \right] D_j, \quad (6)$$

where  $\mu_0$  is the effective boson chemical potential,  $g = g_0$  for the unitary case corresponding to two hyperfine states, and  $g = 2g_0$  for a non-unitary case corresponding to a single hyperfine state. When the composite Boson interactions are dominant the Thomas–Fermi (TF) approximation leads to  $|\mathbf{D}(\mathbf{R}, 0)| = g^{-1/2}[\mu_0 - 2U_{\text{ext}}(\mathbf{R})]^{1/2}$  for  $\mu_0 \geq 2U_{\text{ext}}(\mathbf{R})$ , and  $|\mathbf{D}(\mathbf{R}, 0)| = 0$ , otherwise. When this approximation fails the initial condition for the time evolution can be obtained by solving Eq. (6) numerically.

For  $t > 0$ , we use the transformation  $R_j(t) = b_j(t)R_j(0)$ , where  $b_j(t)$  are scaling factors satisfying, [17, 18]

$$\frac{d^2 b_j(t)}{dt^2} = \frac{\omega_{j,0}^2}{A(t)b_j(t)} \quad (7)$$

with initial conditions  $b_j(t < 0) \equiv 1$  for all  $j$ , and  $A(t) = b_x(t)b_y(t)b_z(t)$ . The  $\mathbf{D}$  vector can be written as

$$D_j(\mathbf{R}(t), t) = \frac{1}{\sqrt{A(t)}} \phi_j(\mathbf{R}(0), t) \exp[iS(\mathbf{R}(t), t)],$$

which upon substitution into Eq. (5) and Eq. (6) at  $t = 0$  leads to

$$S(\mathbf{R}(t), t) = S_0(t) + M \sum_k \frac{R_k^2(t)}{b_k(t)} \frac{db_k(t)}{dt}. \quad (8)$$

For a cigar-shaped trapping potential with axial symmetry ( $\epsilon \equiv \omega_z(0)/\omega_\perp(0) \ll 1$  and  $\omega_\perp \equiv \omega_x = \omega_y$ ),  $D_j(\mathbf{R}, t)$  becomes

$$D_j(\mathbf{R}, t) \approx \frac{\exp[iS(\mathbf{R}, t)]}{\sqrt{1 + \lambda^2}} D_j(\bar{\mathbf{R}}, 0), \quad (9)$$

where  $\bar{R}_k = R_k/b_k(t)$  are scaled coordinates, and  $\lambda \equiv \omega_\perp(0)t$  is the dimensionless time. The result for  $s$ -wave is formally identical to that of Eq. (9) with the substitution  $D_j \rightarrow \Psi$ , where  $\Psi$  represents the scalar order parameter.

The matter-wave interference of two spatially separated condensates (without tunneling) is described by

$$\Phi_{\text{tot}}(\mathbf{R}, t) = \Phi_L(\mathbf{R}, t) + \Phi_R(\mathbf{R}, t), \quad (10)$$

where  $\Phi_P \propto i \sum_j D_{j,P} \sigma_j \sigma_y$  denotes the pair wavefunction of Fermi condensates in the left [ $P = L(+)$ ] or right [ $R(-)$ ] traps. Here, a coordinate system is chosen such that the trap centers lie at  $(-W/2, 0, 0)$  and  $(W/2, 0, 0)$ , where  $W$  is the distance between the traps. We consider the case of two identical cigar shaped Fermi condensates, with the weakest confinement along the  $\mathbf{z}$  axis, just like the experiment in Bose systems [1]. In this case, the time evolution of the two independent Fermi condensates is described by

$$D_{j,P}(\mathbf{R}, t) = \frac{\exp[iS(\mathbf{R} \pm W\hat{\mathbf{x}}/2, t)]}{\sqrt{1 + \lambda^2}} D_j(\bar{\mathbf{R}} \pm W\hat{\mathbf{x}}/2, 0),$$

Thus, for any single run of the experiment, the particle density  $n(\mathbf{R}, t) \equiv |\Phi_{\text{tot}}(\mathbf{R}, t)|^2$  is

$$n(\mathbf{R}, t) \propto |\mathbf{D}_L(\mathbf{R}, t)|^2 + |\mathbf{D}_R(\mathbf{R}, t)|^2 + 2\text{Re} \left[ \frac{\mathbf{D}^\dagger(\bar{\mathbf{R}} + W\hat{\mathbf{x}}/2, 0) \cdot \mathbf{D}(\bar{\mathbf{R}} - W\hat{\mathbf{x}}/2, 0)}{\sqrt{A(\lambda)A(\lambda)}} e^{i\chi} \right], \quad (11)$$

where the phase  $\chi(\mathbf{R}, t) = S(\mathbf{R} + W\hat{\mathbf{x}}/2, t) - S(\mathbf{R} - W\hat{\mathbf{x}}/2, t) + \chi_0$ , and  $\chi_0$  is the initial relative phase of the two clouds. The result for  $s$ -wave is formally identical to that of Eq. (11) with the substitution  $D_j \rightarrow \Psi$ .

In the case where both Fermi condensates are in unitary states,  $\mathbf{D}$  is essentially a real vector with an overall phase, and  $n(\mathbf{R}, t)$  shows an angular dependence controlled by the dot product in Eq. (11). When the two order parameters are parallel, this term is maximal and the interference pattern is most visible (Fig. 2). However if the  $\mathbf{D}$  vectors are perpendicular, fringes are absent at all times (Fig. 3). Therefore, in the unitary case the existence and intensity of interference fringes are very sensitive to the relative orientation of the vector order parameters.

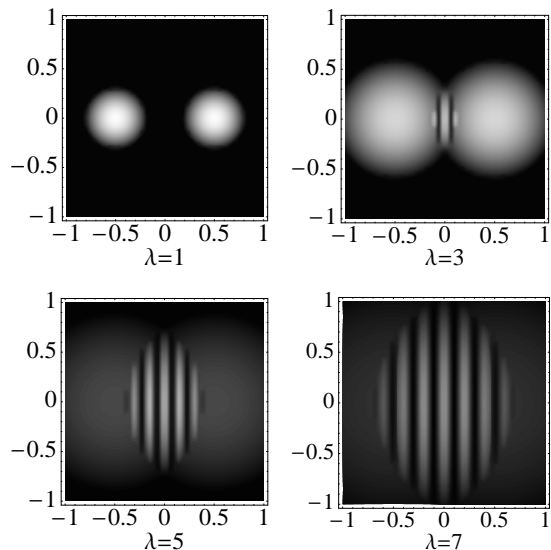


FIG. 2: Interference pattern versus dimensionless time  $\lambda$  for unitary  $p$ -wave Fermi condensates in the BEC limit involving two hyperfine states (cross section view). Each condensate is initially trapped in a cigar-shaped potential with  $\mathbf{D}_L^\dagger \parallel \mathbf{D}_R$ . The patterns are similar for atomic scalar bosons, and for  $s$ -wave and single hyperfine state  $p$ -wave fermions.

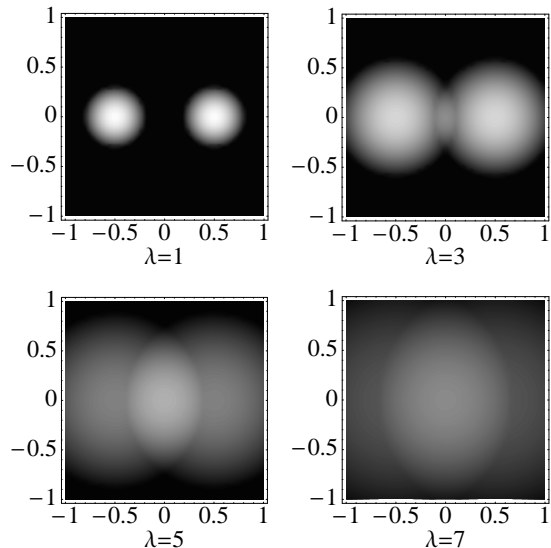


FIG. 3: Same plots as in Fig. 2, but with  $\mathbf{D}_L^\dagger \perp \mathbf{D}_R$ .

When only one hyperfine state is occupied, the  $\mathbf{D}$  vector has a fixed form  $A(1, i, 0)$ . Without this pseudospin space rotational degree of freedom, the angular dependence of the interference pattern disappears and fringes are present in all experimental realizations. This result is similar to the  $s$ -wave case where the order parameter is a complex scalar.

Before concluding, we would like to mention two im-

portant points. First, away from the BEC limit the kinetic energy term in Eq. (4) is

$$- \sum_{i,j,m_\ell} \frac{\nabla_i \nabla_j}{2M_{m_\ell}^{i,j}} D_{j,m_\ell},$$

thus acquiring a mass anisotropy  $M_{m_\ell}^{i,j} = M/c_{m_\ell}^{i,j}$ , which is directly related to the anisotropy of the Ginzburg–Landau coherence length  $\xi_{ij}$ . Here, we use the basis of spherical harmonics  $Y_{1,m_\ell}$  and define  $D_{j,m_\ell}$  by  $d_j(\mathbf{r}, \mathbf{r}') = \sum_{m_\ell} D_{j,m_\ell}(\mathbf{R}) \eta_{0,m_\ell}(x) Y_{1,m_\ell}(\hat{\mathbf{x}})$ . For a weak trapping potential, the coefficient  $c_{m_\ell}^{i,j}$  becomes

$$c_{m_\ell}^{i,j} = \sum_{\mathbf{k}, m'_\ell} \left\{ \left[ \frac{X(\mathbf{k})}{4E^2(\mathbf{k})} - \frac{\beta Y(\mathbf{k})}{16E(\mathbf{k})} \right] \delta_{m_\ell, m'_\ell} \delta_{i,j} + \kappa_{m_\ell, m'_\ell}^{i,j} \frac{\beta^2 \mathbf{k}^2 X(\mathbf{k}) Y(\mathbf{k})}{32mE(\mathbf{k})} \right\} \phi^2(k), \quad (12)$$

where  $E(\mathbf{k}) = \xi_{1,\mathbf{k}} + \xi_{2,\mathbf{k}}$ ,  $\xi_{\alpha,\mathbf{k}} = \mathbf{k}^2/2m - \mu_\alpha$ ,  $X(\mathbf{k}) = \tanh(\beta\xi_{1,\mathbf{k}}/2) + \tanh(\beta\xi_{2,\mathbf{k}}/2)$ , and  $Y(\mathbf{k}) = \text{sech}^2(\beta\xi_{1,\mathbf{k}}/2) + \text{sech}^2(\beta\xi_{2,\mathbf{k}}/2)$ . The symmetry function  $\phi(k)$  is defined by  $V(\mathbf{k}, \mathbf{k}') = \int d\mathbf{x} V(\mathbf{x}) \exp[i(\mathbf{k} - \mathbf{k}') \cdot \mathbf{x}] = V\phi(k)\phi(k') Y_{1,m_\ell}(\hat{\mathbf{k}}) Y_{1,m'_\ell}^*(\hat{\mathbf{k}}')$ , and the angular average

$$\kappa_{m_\ell, m'_\ell}^{i,j} = \int d\hat{\mathbf{k}} \hat{k}_i \hat{k}_j Y_{1,m_\ell}(\hat{\mathbf{k}}) Y_{1,m'_\ell}^*(\hat{\mathbf{k}}).$$

When the order parameter is characterized by one  $Y_{1,m_\ell}$  with  $m_\ell$  fixed,  $\kappa$  is diagonal in both  $m_\ell$  and  $i$ , hence  $c_{m_\ell}^{i,j} = c_{j,m_\ell} \delta_{i,j}$ . This mass anisotropy reflects the higher angular momentum ( $p$ -wave) nature of the order parameter for paired fermions, and it is completely absent in  $s$ -wave Fermi and atomic Bose condensates.

This effective mass anisotropy has a non-trivial influence on the time evolution of condensates after release from the trap. Making the scale transformation  $R'_j = R_j \sqrt{M_{j,m_\ell}}$ ,  $\omega'_j = \omega_j / \sqrt{M_{j,m_\ell}}$ , we conclude that the cloud expansion predominantly occurs in the strongest confined direction in the scaled space. Thus, the time evolution of a Fermi condensate initially trapped in an axially symmetric potential with sizes  $L_x = L_y < L_z$  leads to an anisotropic cross section of the cloud at any time after release when  $M_x \neq M_y$  ( $\xi_x \neq \xi_y$ ). In Fig. 4, we show the cloud anisotropy ratio as a function of the effective mass anisotropy ratio.

Second, in the discussion above we assume a symmetric interaction in pseudospin space, i.e.,  $V_{1111}$ ,  $V_{1212}$  and  $V_{2222}$  are identical. However, experimental results for  $p$ -wave Feshbach resonances show a small but finite separation in different channels [14]. Different interactions in pseudospin space do not affect dramatically our derivation or results. When the different interactions are absorbed into an effective  $\mathbf{D}$  vector, an equivalent procedure leads to equations similar to Eqs.(5) and (6).

In conclusion, we considered a Fermi condensate consisting of two hyperfine states with  $s$ -wave and  $p$ -wave

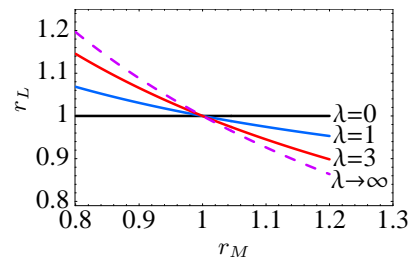


FIG. 4: Cloud anisotropy ratio  $r_L = L_x/L_y$  as a function of effective mass anisotropy ratio  $r_M = M_x/M_y$  at time  $\lambda$  (Solid lines). Dashed line indicate the saturated behavior at  $\lambda \rightarrow \infty$ .

interactions, and derived equation of motion for  $p$ -wave case in a vector boson representation near the BEC limit. We found that the quantum interference of two  $p$ -wave Fermi condensates has a polarization effect due to the vector nature of the order parameter. This effect is absent in strongly coupled (BEC)  $s$ -wave Fermi superfluids, as well as in scalar atomic Bose systems. Furthermore, we observed that different orbital symmetries of the vector order parameter produce anisotropic effective masses (coherence lengths). For a cigar-shaped cloud with an isotropic cross section, the cloud expansion becomes anisotropic at any time after release from the trap when the effective masses are anisotropic. Thus, the orbital symmetry of the order parameter for  $p$ -wave condensates can be probed via single cloud expansions.

- 
- [1] Y. Shin *et al.*, Phys. Rev. Lett. **92**, 050405 (2004).
  - [2] T. Schumm *et al.*, Nature Physics **1**, 57 (2005).
  - [3] S. Fölling *et al.*, Nature **434**, 481 (2005).
  - [4] K. E. Strecker, G. B. Partridge, and R. G. Hulet, Phys. Rev. Lett. **91**, 080406 (2003).
  - [5] M. Greiner, C. A. Regal, and D. S. Jin, Nature (London) **426**, 537 (2003).
  - [6] M. W. Zwierlein *et al.*, Phys. Rev. Lett. **91**, 250401 (2003).
  - [7] M. Bartenstein *et al.*, Phys. Rev. Lett. **92**, 120401 (2004).
  - [8] T. Bourdel *et al.*, Phys. Rev. Lett. **93**, 050401 (2004).
  - [9] J. Kinast *et al.*, Phys. Rev. Lett. **92**, 150402 (2004).
  - [10] C. A. R. Sá de Melo, M. Randeria, and J. R. Engelbrecht, Phys. Rev. Lett. **71**, 3202 (1993).
  - [11] M. Iskin and C. A. R. Sá de Melo, Phys. Rev. Lett. **96**, 040402 (2006).
  - [12] C. A. Regal, C. Ticknor, J. L. Bohn, and D. S. Jin, Phys. Rev. Lett. **90**, 053201 (2003).
  - [13] J. Zhang *et al.*, Phys. Rev. A **70**, 030702(R) (2004).
  - [14] C. H. Schunck *et al.*, Phys. Rev. A **71**, 045601 (2005).
  - [15] K. Gunter *et al.*, Phys. Rev. Lett. **95**, 230401 (2005).
  - [16] I. V. Tokatly, Phys. Rev. A **70**, 043601 (2004).
  - [17] Yu. Kagan, E. L. Surkov, and G. V. Shlyapnikov, Phys. Rev. A **54**, R1753 (1996).
  - [18] Y. Castin and R. Dum, Phys. Rev. Lett. **77**, 5315 (1996).